

## Supporting information

### **Multi-functional Micromotor: Microfluidic Fabrication and Water Treatment**

#### **Application**

*Anqi Chen<sup>‡</sup>, Xue-hui Ge<sup>‡</sup>, Jian Chen, Liyuan Zhang\*, Jian-Hong Xu\**

#### **The details of the microfluidic device**

We use the double-core capillary microfluidic device to form the droplets and then collect them into the petri-dish. The tip of the double-core capillary is tipped with 50  $\mu\text{m}$  of each core. The joint of the tubes, capillaries and chips are sealed by glues. Other devices are micropipette puller (P-97, SUTTER Co. Ltd., USA) for pulling the capillary into a tip, micro-syringe pumps (LP01-1B, Longer Precision Pump Co. Ltd.) for pumping the liquids, and the optical microscope (BX61, Olympus Co.Ltd) for taking microphotographs and movies. We take the Scanning Electronic Microscopy (SEM) images through SEM machine (TM3000, Hitachi Co. Ltd.). The ultraviolet UV-visible spectrophotometer (UV-2450, Shimadzu Co. Ltd.) is used to achieve the concentration of the methylene blue waste water solutions. The wavelength for measuring is 664 nm.

#### **The disperse of the TiO<sub>2</sub> nanoparticles**

The TiO<sub>2</sub> nanoparticles are dispersed in the liquid paraffin. To find out whether they disperse into the ETPTA phase, we add liquid paraffin and ETPTA in one glass well and add 2 wt.% TiO<sub>2</sub> nanoparticles. After mixing them in the microwave machine, the nanoparticles disperse in the mixtures well (**Figure S1a**). After keeping for 24 hours, we could find that the liquid paraffin and ETPTA separate and the TiO<sub>2</sub> nanoparticles disperse only in the liquid paraffin phase and the interface between these two immiscible phases. The SEM images of the micromotors with TiO<sub>2</sub> nanoparticles are also shown in **Figure S1b**.

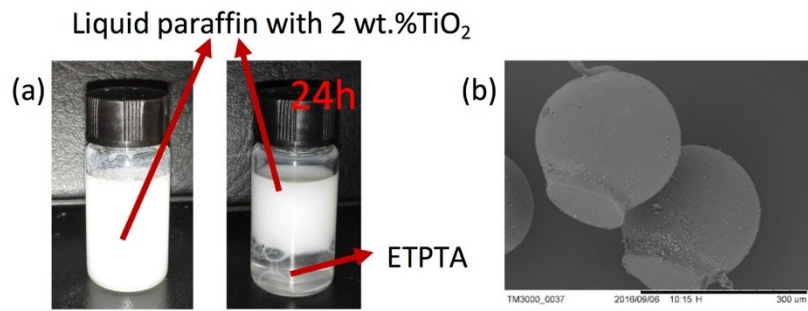


**Figure S1.** The supporting images of the photo-catalyst process. (a) The dispersion of TiO<sub>2</sub> nanoparticles. (b) The SEM images of what micromotor containing TiO<sub>2</sub> nanoparticles .

### The motor without magnetic nanoparticles

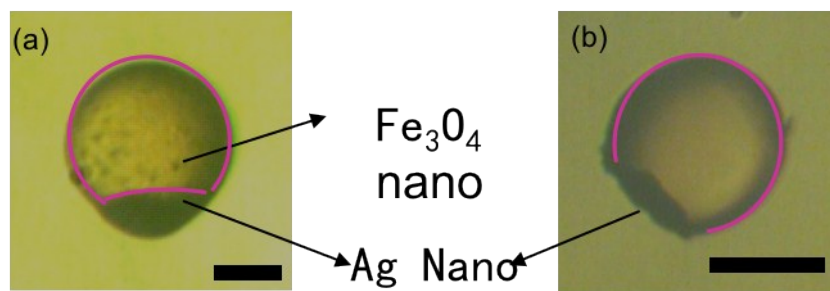


**Figure S2.** (a) Micromotor with magnetic nanoparticles. There are black dots in the upper semi-spherical part (ETPTA part). (b) Micromotor without magnetic nanoparticles. The ETPTA part is clean. The scale bar represents 100  $\mu\text{m}$ .

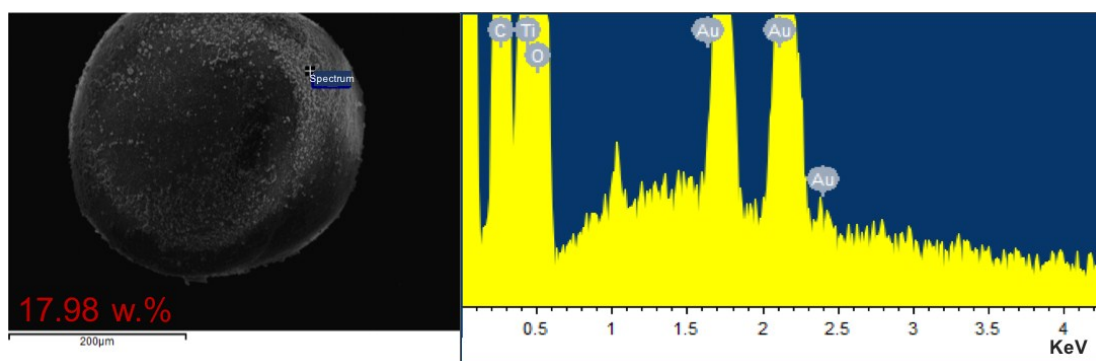


**Figure S3.** (a) SEM image of micromotor containing TiO<sub>2</sub> nanoparticles. (b) The energy spectrum of Ag nanoparticles in the surface.

## The Ag concentration

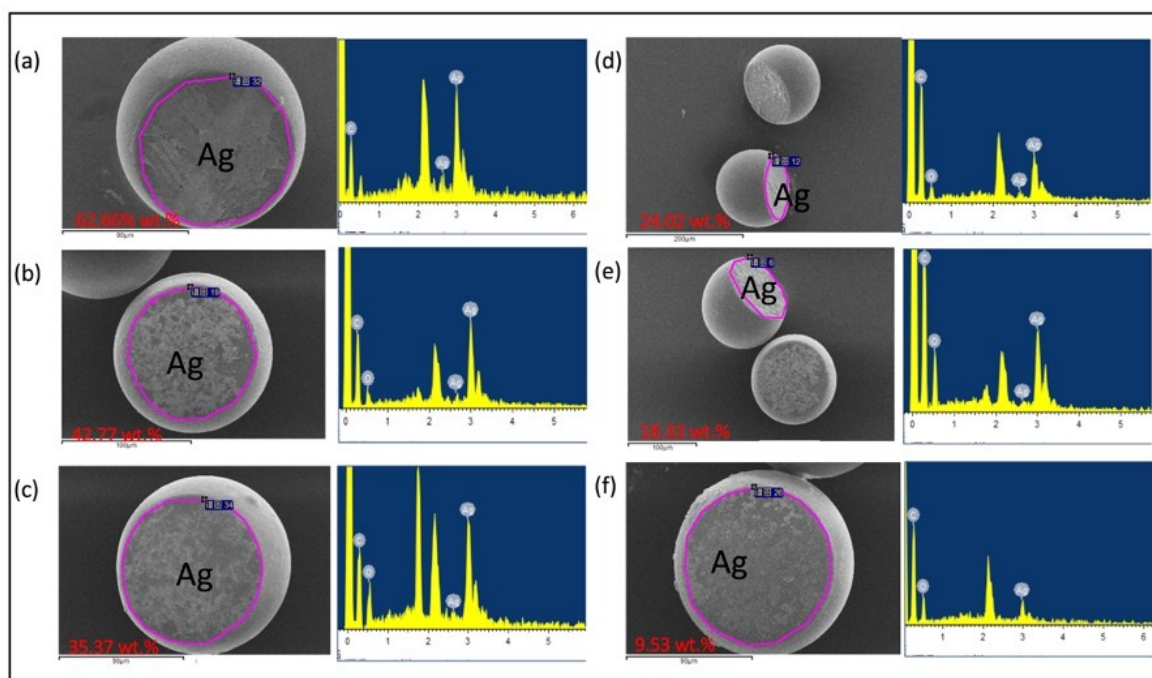


**Figure S4.** The energy spectrum of Ag nanoparticles in the surface.

## Two methods to improve the Ag concentration at the interface

To increase the Ag concentration, two methods are used in the manuscript: increase the length of the collecting tube before solidifying the water-oil Janus droplet; Increase the hydrophobicity of Ag nanoparticles.

The improved microfluidic device with longer collecting tube could be found in **Figure S5**. By prolonging the residence time of droplets in the outlet tube, the adsorption time of Ag nanoparticles to the water-oil interface in the outlet section increases to increase the Ag loading efficiency on the interface.

In order to increase the surface loading of silver in the microparticle plane, the silver nanoparticles were hydrophobically modified by reference<sup>[1]</sup>.

The modified process is: 1 mmol / L 1-octanethiol n-heptane solution and 1 mmol / L n-octadecanethiol n-heptane solution were prepared and mixed in a volume ratio of 1: 2 to prepare a modifier. A small amount of silver was immersed in an excess of the modifier for

---

30 minutes, washed with n-heptane three times to remove residual thiol molecules, and spontaneously evaporated heptane to obtain modified silver nanoparticles. The modified silver nano-particles were characterized by Infrared Spectrum (IR) and photographed to measure the contact angle of the water droplets on the silver surface.

From **Figure S6**, the infrared spectra showed that the hydroxyl groups of the silver surface decreased and the carbon chain increased, and the contact angle of the silver surface showed that the hydrophobicity of silver was greatly enhanced. The contact angle changes from  $36.8^\circ$  (meaning the hydrophilicity) to  $138.0^\circ$  (meaning the hydrophobicity).

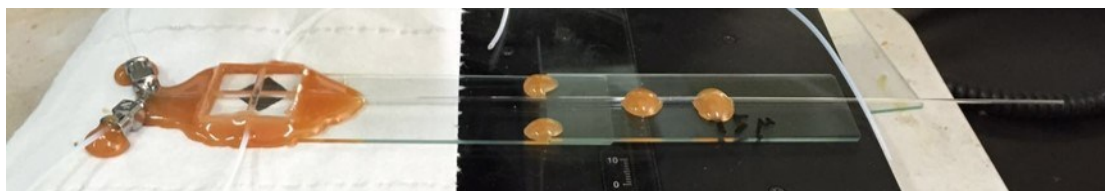


**Figure S5.** The photo of the microfluidic device with a long collecting tube.

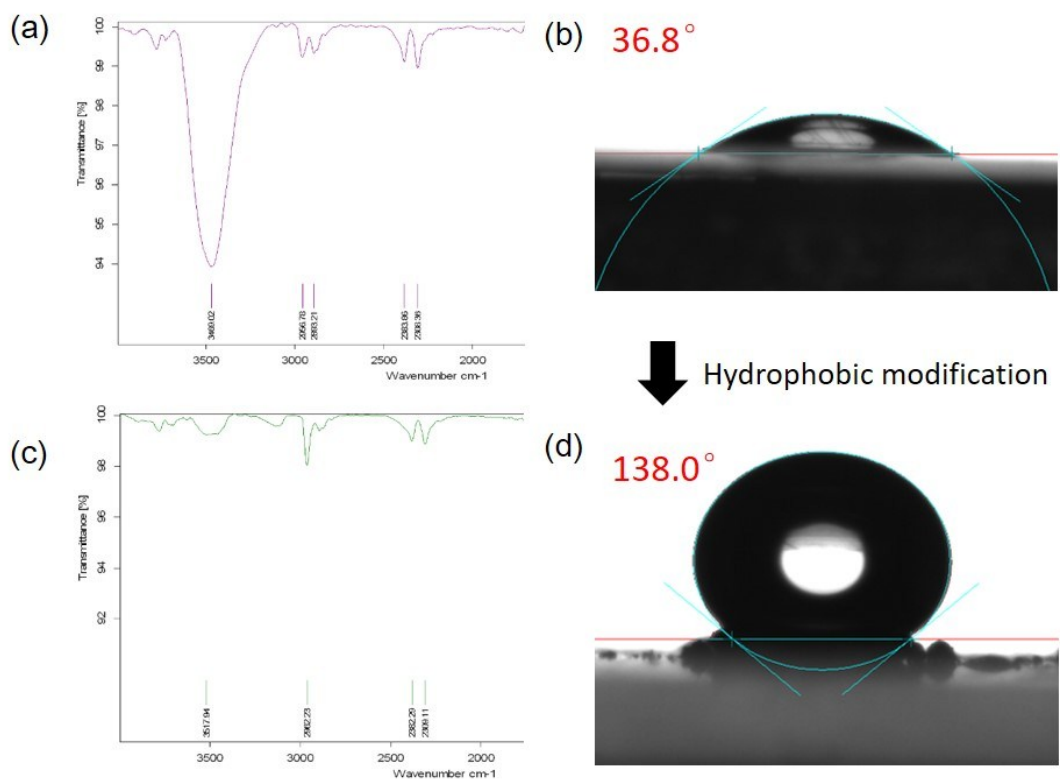


**Figure S6.** The surface modification on the Ag nanoparticles. (a) Before modification: The IR before modification shows the hydroxyl groups of the silver surface. (b) The hydrophilic ability of Ag nanoparticles result in the contact angle of 36.8°. (c) After modification: The IR after modification shows the increased carbon chain while decreased hydroxyl groups. (d) The hydrophobic ability of Ag nanoparticles result in the contact angle of 138.0°.

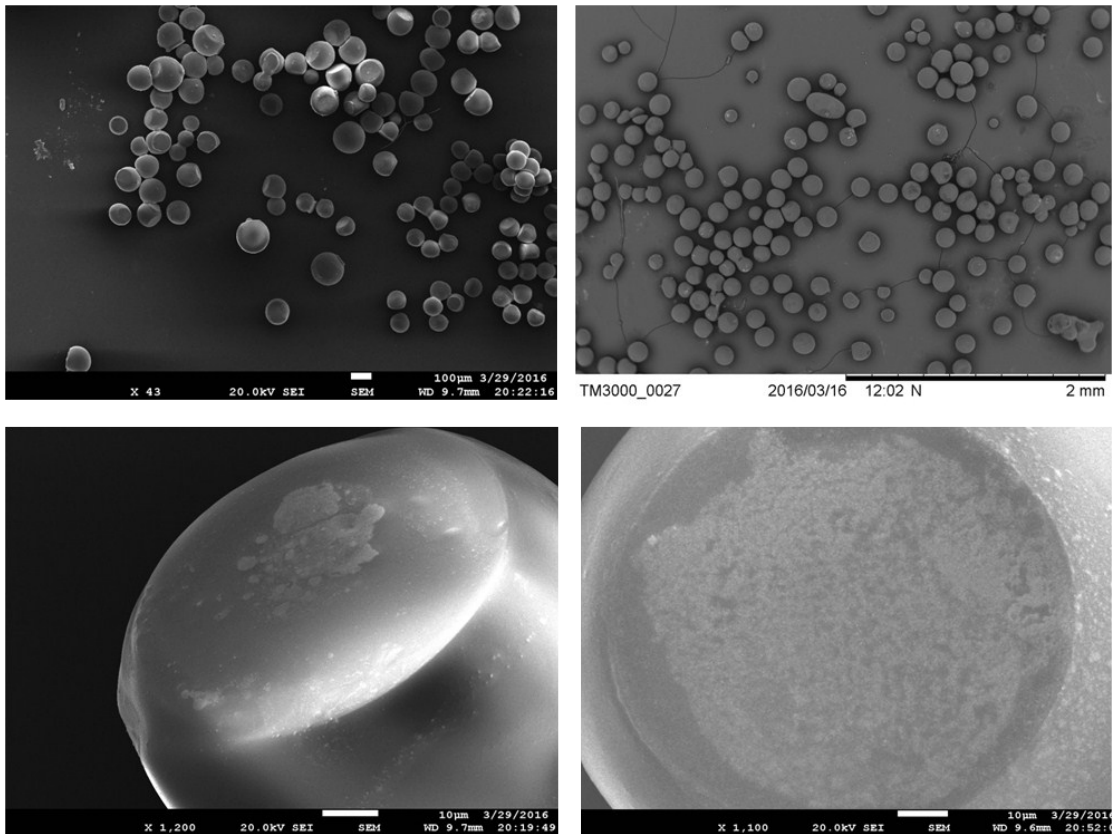
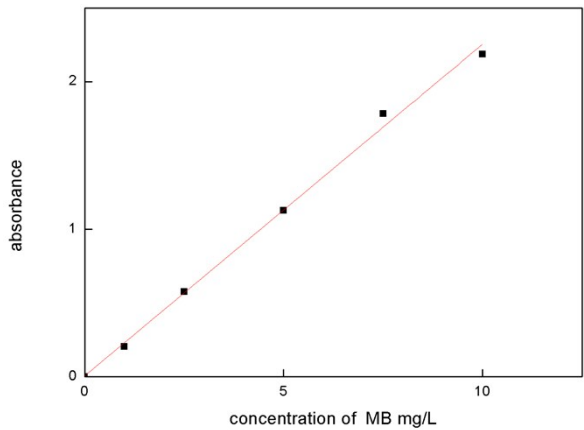


**Figure S7.** Electron micrographs of silver samples prepared by long outlet channel modified silver

**The standard absorption curve**

Pure water, 2.5mg / L, 5mg / L, 7.5mg / L and 10mg / L of methylene blue were respectively prepared and the absorbance at each concentration was measured with a ultraviolet-visible spectrophotometer. The standard curve (**Figure S8**) shows that the absorbance has a linear relationship with the concentration of methylene blue.



---

**Figure S8.** The standard absorption curve of the methylene blue.

Reference:

- [1] Martin Jahn, Sophie Patze, Thomas Bocklitz, Karina Weber, Dana Cialla-May, Jürgen Popp, *Anal. Chim. Acta*, **2015**, *860*, 43-50.